

## Solvation and Evolution Dynamics of an Excess Electron in Supercritical CO<sub>2</sub>

Zhiping Wang,<sup>1</sup> Jinxiang Liu,<sup>1</sup> Meng Zhang,<sup>1</sup> Robert I. Cukier,<sup>2</sup> and Yuxiang Bu<sup>1,\*</sup>

<sup>1</sup>The Center of Molecular Modeling & Simulation, Institute of Theoretical Chemistry, Shandong University, Jinan, 250100, People's Republic of China.

<sup>2</sup>Department of Chemistry, Michigan State University, East Lansing, Michigan 48824, USA

(Received 20 October 2011; revised manuscript received 8 February 2012; published 17 May 2012)

We present an *ab initio* molecular dynamics simulation of the dynamics of an excess electron solvated in supercritical CO<sub>2</sub>. The excess electron can exist in three types of states: CO<sub>2</sub>-core localized, dual-core localized, and diffuse states. All these states undergo continuous state conversions via a combination of long lasting breathing oscillations and core switching, as also characterized by highly cooperative oscillations of the excess electron volume and vertical detachment energy. All of these oscillations exhibit a strong correlation with the electron-impacted bending vibration of the core CO<sub>2</sub>, and the core-switching is controlled by thermal fluctuations.

DOI: 10.1103/PhysRevLett.108.207601

PACS numbers: 79.05.+c, 33.15.Ry, 61.20.Ja, 82.33.De

The discovery of excess electron (EE) solvation in various media has implications in biology, chemistry, atmospheric science, astrophysics, and cluster science [1–7]. When high-energy radiation or an electrode discharge passes through some medium, solvent-bound electrons may be formed. Such electrons exist mainly in three forms: solvent-bound valence anions, cavity-type solvated states, and diffuse states, depending on the medium's electronic properties, heterogeneity, and degree of aggregation. Although solvated states and solvent-bound valence anions are well known, with clearly characterized structures [8–17], EE delocalization has been relatively little explored. Usually, when an EE is added into a fluid, it is absorbed first as a delocalized state, and then may evolve to a localized state. Even if a localized state is formed, it is generally short-lived and readily converts into other localized or diffuse states before being scavenged or reacting [8]. This scenario is different from what occurs in gas phase clusters. Information about conversions among localized and diffuse states or the evolution dynamics of solvent-bound EEs is very scarce.

Supercritical CO<sub>2</sub> (scCO<sub>2</sub>), a nontoxic, nonflammable, easily recyclable, and environmentally friendly solvent, appears to be a promising medium for charge-transfer reactions, and for reprocessing nuclear waste [18–31]. Unlike polar water, ammonia, alcohols, and apolar or weakly polar organic solvents, a CO<sub>2</sub> molecule is bond polar but overall apolar and has a large negative gas phase vertical electron affinity (−0.9 eV) [26,27], indicating that it can not directly bind an EE. However, bending vibrations can lead to a transient dipole for each CO<sub>2</sub>, and thus to its potential to bind an EE. Further, solvation in liquid or clusters or adsorption on solid surfaces could improve its EE-binding ability by stabilizing the EE-bound CO<sub>2</sub> motifs [32–41]. In particular, in the supercritical state, the CO<sub>2</sub> molecule is marginally nonlinear with an average angle of ∼174°, and thus possesses a small dipole moment [42–47]. Thus, scCO<sub>2</sub>

could bind an EE through bending and solvation. The exclusive formation of two kinds of cored valence anions in neat scCO<sub>2</sub> and gaseous clusters: monomer-core (CO<sub>2</sub><sup>−</sup>) and dimer-core (C<sub>2</sub>O<sub>4</sub><sup>−</sup>) anions [24–31,35–41] has been suggested experimentally and theoretically. To our knowledge, however, their EE states have not yet been elucidated in finite CO<sub>2</sub> systems. Although a lot of structural and electronic information about EE-bound motifs has been acquired experimentally and theoretically for charged scCO<sub>2</sub> or liquid CO<sub>2</sub> and gaseous (CO<sub>2</sub>)<sub>n</sub><sup>−</sup> ( $n = 1–17$ ) anion clusters that suggests the existence of two kinds of core ions (CO<sub>2</sub><sup>−</sup> versus C<sub>2</sub>O<sub>4</sub><sup>−</sup>) and possible switching between them, subject to the (CO<sub>2</sub>)<sub>n</sub><sup>−</sup> size [26–29,35–41], the relevant dynamical information is scarce. Also, the degree of localization of an EE in scCO<sub>2</sub> needs clarification, because it is closely associated with the assignment of various possible states of the solvent-bound EE and its evolution dynamics.

Microscopic level information on an EE in scCO<sub>2</sub> is experimentally difficult to obtain because of the ultrafast dynamics and short lifetimes of the solvated EE states. In this work, we conducted *ab initio* molecular dynamics (AIMD) simulation studies of an EE-absorbed in dense, liquidlike scCO<sub>2</sub> with the aims of exploring the EE states and time evolution dynamics, and providing a microscopic level understanding of the interactions of a quasifree EE with scCO<sub>2</sub>.

AIMD simulations were performed on a supercritical system ( $T = 314.1$  K,  $\rho_c = 0.837$  g/cm<sup>3</sup>) consisting of 60 CO<sub>2</sub> molecules in a periodically repeated cubic cell (cell parameter of 17.37 Å) and an EE. This system will be referred to as EE@scCO<sub>2</sub>. Spin unrestricted calculations were carried out for 9 ps after the addition of an EE to the neutral system that was preequilibrated for 3 ps. The system temperature was kept around 314.1 K by the use of a Nosé-Hoover chain of thermostats within the canonical *NVT* ensemble. The  $\Gamma$  point was used in the Brillouin zone sampling. A 1 fs time step was used to ensure good control of the conserved quantities.

The nonlocal Becke, Lee, Yang, and Parr exchange-correlation function and a double numerical plus polarization basis set [48,49] were used in the AIMD simulations. The finite range cutoff of the atomic basis set was 3.7 Å and self-consistent field convergence threshold was  $10^{-6}$ . The electrostatic potential was evaluated by solving Poisson's equation [50] with cutoff optimization in a completely numerical approach for the charge density. The spin states of electrons in a single unit cell were changed from singlet to doublet upon the addition of an EE to the equilibrated neutral system, and the total charge of the unit cell was reset to  $-1$ . In addition, two larger cells containing 90 and 125  $\text{CO}_2$  molecules with different initial configurations were also AIMD simulated for EE@sc $\text{CO}_2$  with similar results. Examinations also indicate that the adiabatic assumption is valid for all these AIMD simulations. We also calculated the vibrational density of states of neutral sc $\text{CO}_2$  and compared it with the Car-Parrinello molecular dynamics results [44]. The agreement is excellent and indicates that the corresponding velocity time correlation function decays by dephasing on about a 0.5 ps time scale [51].

Upon an attachment to the preequilibrated neutral sc $\text{CO}_2$ , an EE enters the lowest of a low-lying unoccupied molecular orbital set (an empty band) consisting of a LUMO of each  $\text{CO}_2$ . This results in the formation of a singly occupied molecular orbital (SOMO) with the EE distributed over several  $\text{CO}_2$  molecules [Fig. 1(a)]. For each  $\text{CO}_2$  participating in binding the EE cooperatively, it binds a part of the EE mainly through its polarization interaction, a distinctly different mechanism from that which operates in water and other solvents, with their polar, dipolar, or electrostatic-based

potentials. Inspection of different starting configurations for EE injection shows similarly diffuse distributions. The average vertical electron affinity of these different starting configurations is about 1.0 eV, indicating that EE capture is thermodynamically favorable. This result is in agreement with the experimental conclusion that liquid  $\text{CO}_2$  is an efficient electron captor [29], and also with the small polarity of sc $\text{CO}_2$  predicted from neutron diffraction experiments and other AIMD simulations [42–47].

One anticipates that the vertically absorbed EE is unstable or metastable and that it rapidly relaxes to a stabilized state. As expected, at an early time of about 20 fs the absorbed EE gradually stabilizes. But, unexpectedly, not all the  $\text{CO}_2$  participate in binding the absorbed EE or promote its further stabilization. Instead, only one  $\text{CO}_2$  dominates the time evolution. The EE cloud becomes localized, gathering around one  $\text{CO}_2$  that acts as a core, and all the other molecules solvate the core-tethered EE [Figs. 1(b) or 1(c)]. Then, as time progresses, the EE cloud expands to a diffuse state, similar to its initial state. This process can be considered as a breathing process, with a period of about 40 fs. Interestingly, the diffuse EE cloud can shrink back to the same core  $\text{CO}_2$ , becoming a localized state, and then expanding to a diffuse state again, with an average breathing period of about 40 fs.

Figure 2(a) displays the EE states at three different times in the range of 8200–8320 fs (Fig. 3), which shows the change of the EE states and the corresponding breathing process and period. This breathing oscillation around the same core can last for 1–3 ps until the EE gathers around a new core (another  $\text{CO}_2$ ) subject to thermally induced configurational fluctuations. This latter core-switching localization process describes a transfer step of the EE from one localized state to another. But, it occurs through a breathing shift pathway

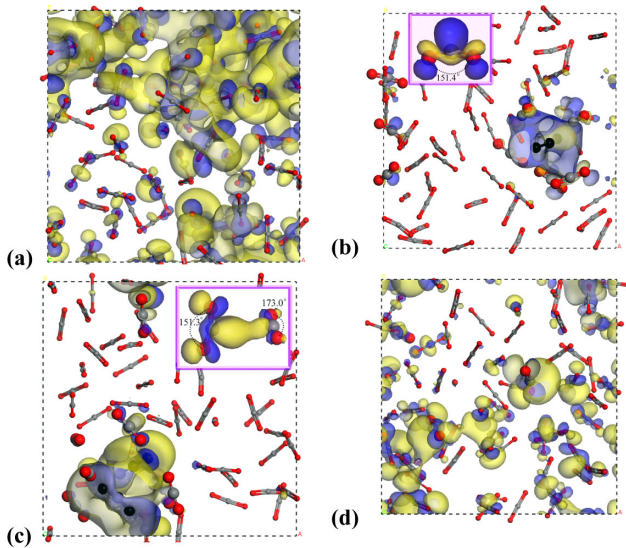


FIG. 1 (color online). (a) SOMO contours of an EE in sc $\text{CO}_2$  in a representative delocalized state, (b), (c) two typical localized states, and (d) A dual-core (quasi) localized state. Surfaces are plotted at an isovalue of 0.003. Notably, the dual-core localized state is not a dimer-core state, because the two cores are separated in the former.

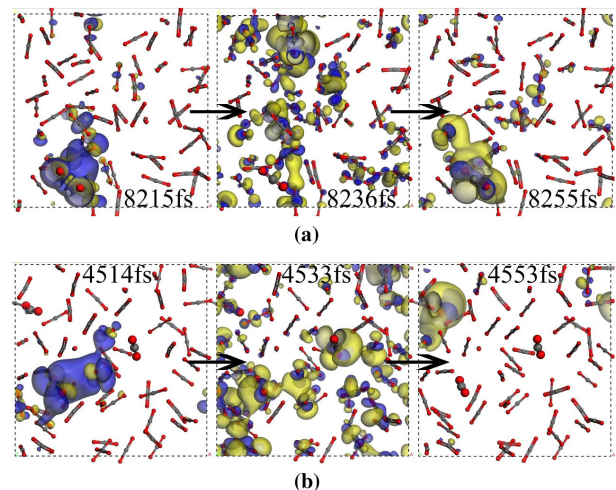


FIG. 2 (color online). SOMO character of the representative snapshots over two arbitrary time intervals extracted from the AIMD simulations. The core  $\text{CO}_2$  molecules are highlighted in ball and stick scheme, and the times are marked on each panel. (a) An arbitrary breathing period. (b) Core-switching shift migration.

instead of a simple donor-to-acceptor one-step transfer. It can be described as a core-switching, breathing shift mechanism [Fig. 2(b)], and is a novel electron transfer mechanism. This complex transfer process generally takes place within about 40–120 fs, about 1–3 times the breathing oscillation period (40 fs) in which some dual-core-based localized states could be observed [Fig. 1(d)] as transitory intermediate states. After core-switching, similar breathing oscillations around the new core continue for some time until the next new core is formed.

To characterize the spatial extent of the EE cloud and depict the breathing oscillation, the volume encapsulated by the 0.03-isovalued spin density surface was calculated for each snapshot configuration, and its time course is displayed in Fig. 3, for an arbitrary time region. Unexpectedly, this parameter exhibits a continuous time oscillation, in complete cooperativity with the breathing oscillation of the EE distributions. Also, we observed a strong correlation of the continuous breathing phenomenon and breathing-shift-based, core-switching migration with the bending vibrations of relevant CO<sub>2</sub> molecules along with stretching-coupled periodic bending vibrations (Fig. 3).

In addition, geometrical characteristics of the breathing oscillation were examined by analyzing the radial distribution functions of the intermolecular C-C distance, intermolecular C-O distance, intramolecular C-O distance, and the angle distribution function of the ∠OCO angle (Fig. 4) for both scCO<sub>2</sub> and EE@scCO<sub>2</sub>. No noticeable changes of the C-C and C-O distances were found in EE@scCO<sub>2</sub> compared with those in neutral scCO<sub>2</sub> [Fig. 4(a)], while a statistical analysis of the bending angle distribution reveals the EE-trapping effect [Fig. 4(b)]. A distinct difference between an EE-binding core CO<sub>2</sub> and an arbitrary neutral CO<sub>2</sub> molecule is that the bending angle distribution of the former becomes wide and its peak shifts considerably toward the small angle region. In combination with the features with which both bending and elongation of a CO<sub>2</sub> increase its electron-binding ability, the breathing motion of the EE cloud arises from stretching-coupled bending vibrations of the CO<sub>2</sub> molecules [35]. The ∠OCO bending vibration

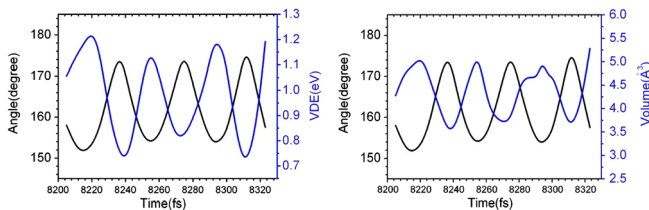


FIG. 3 (color online). Oscillation behavior of the VDE (left panel), the volume surrounded by the spin density isovalue (0.03) surfaces of EE (right panel) for an arbitrary time period (8200–8320 fs), and their cooperative relationships with the ∠OCO angle change. Note for both panels from left to right, the curves starting from the lower correspond to the angle change, while those starting from the upper correspond to VDE and volume changes, respectively.

also exhibits regular oscillations in its time evolution, in cooperativity with the continuous breathing oscillation and core-switching (see Figs. 3 and 5). For a core molecule, the ∠OCO angle oscillates in a range of 150°–180° with an average of about 165°, while a surrounding CO<sub>2</sub> (uncharged, similar to a CO<sub>2</sub> in neutral scCO<sub>2</sub>) oscillates between 170°–180° with an average value at around 175°, in agreement with experimental observations and other AIMD simulations on neutral scCO<sub>2</sub> [42–47].

Dual-core (two separated single cores) states were observed in the core-switching process, but the dimer core, (O<sub>2</sub>C-CO<sub>2</sub>)<sup>-</sup>, did not occur, in indirect agreement with the cluster-model-based assertion that the monomer core (CO<sub>2</sub><sup>-</sup>) is preferred in (CO<sub>2</sub>)<sub>n</sub><sup>-</sup> clusters, for  $n = 7–13$  [38–40]. This is understandable. Since scCO<sub>2</sub> is flexible, due to thermal fluctuations, the EE-binding motif is unlikely to possess a well-defined structure [28]. As revealed by photoelectron imaging, the orbital nature of the two competing core ions is similar in (CO<sub>2</sub>)<sub>n</sub><sup>-</sup> ( $n = 4–9$ ) anion clusters, and the dimer-core anion electronic structure can be expressed as a linear combination of two monomeric contributions [40,41], implying the dual cores observed in this AIMD simulation. The existence of a dimer core relies on symmetric solvent configurations, especially in the first solvent shell. However, such configurations are unlikely to form in the dynamical process, and thus the nonoccurrence of the dimer core is reasonable. Furthermore, monomer-core localized electron states can not be simply described as a CO<sub>2</sub><sup>-</sup> valence anion because only a part of the EE is localized on the CO<sub>2</sub> core.

To characterize the stability of an EE in scCO<sub>2</sub>, vertical detachment energies (VDEs) were determined for selected snapshots. Figure 3 shows that VDEs fall in the range 0.70–1.24 eV with regular oscillations along the trajectory that are highly cooperative with the bending vibration oscillations and thus continuous EE breathing oscillations.

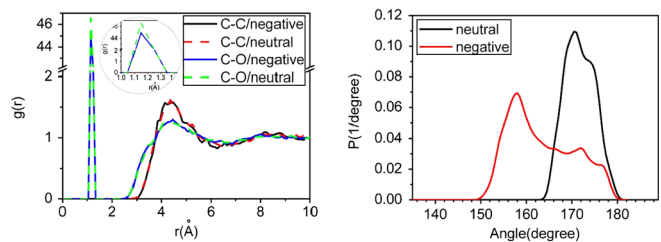


FIG. 4 (color online). (a) Radial distribution functions and (b) angular distribution function of the intramolecular ∠OCO of the core CO<sub>2</sub>, for the neutral and the EE-absorbed scCO<sub>2</sub>. Addition of an EE to scCO<sub>2</sub> has a noticeable effect on the ∠OCO distribution. The statistical analyses are made on the basis of the trajectory data in the last 3 ps of the AIMD simulations for EE@scCO<sub>2</sub> and scCO<sub>2</sub>, respectively. Note that in the left panel, the curve with a higher peak at about 4 Å corresponds to the C-C distance distribution, while other curves correspond to the C-O distance distribution. In the right panel, the curve with a wide peak corresponds to the negative.



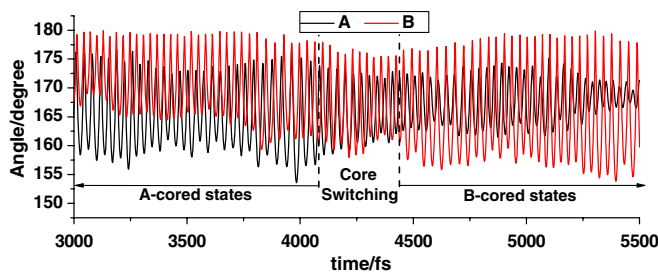


FIG. 5 (color online). Oscillation of the  $\angle\text{OCO}$  bending vibration for two arbitrary  $\text{CO}_2$  (A/black curve and B/red curve) that are the cores, in turn, which absorb an EE as localized states. Core switching was observed at 4100–4400 fs, which corresponds to the transfer of the EE from the A to the B cored localized state, mainly experiencing 4–6 oscillation periods, and thus describable as a core-switching breathing shift mechanism.

In general, the diffuse EE states have small VDE values (0.7–0.8 eV), while the localized EE states have large ones (1.1–1.2 eV). The small difference ( $\sim 0.5$  eV) between the two limits (fully diffuse versus localized) and frequent oscillations suggest a large mobility for the EE, and also a propensity to escape from  $\text{scCO}_2$ .

In traditional studies based on cluster models, VDEs are generally calculated only at the minimum energy geometries. In reality, a VDE varies with the molecular geometry and bulk fluctuations. Consequently, VDEs of an EE in  $\text{scCO}_2$  should correspond to a broad peak in a photoelectron spectrum, in the range  $\sim 0.7$  to 1.3 eV. The experimental VDE values of 1.2–1.7 eV on monomer-cored  $\text{CO}_2^- \cdot (\text{CO}_2)_n$  cluster anions indirectly support our conclusion [41].

We also performed another AIMD simulation at a high temperature supercritical state ( $T = 373.0$  K,  $\rho_c = 0.800$  g/cm<sup>3</sup>). The time-dependent  $\angle\text{OCO}$  angle changes of two arbitrary  $\text{CO}_2$  molecules that do not participate in binding an EE and two core  $\text{CO}_2$  molecules in  $\text{EE@scCO}_2$ , which bind the EE, extracted from two temperature trajectories are shown in Fig. 6. Two points are revealed by comparing the four oscillation curves (charged versus uncharged, 314.1 versus 373.0 K): (1) Charging considerably elongates oscillation periods of the  $\angle\text{OCO}$  angle bending vibration, especially for the high temperature system. (2) High temperature inhibits the bending oscillations of the charged systems, as is clear from the oscillation periods ( $\sim 40$  fs/314.1 K versus 50–60 fs/373.0 K) of the charged core  $\text{CO}_2$ . Correspondingly, oscillations of the EE distributions and VDEs also slow down. Thus, both charging and raising the temperature can inhibit the bending vibrations of  $\text{CO}_2$  molecules and the oscillations of the EE cloud.

As an additional note, although low-energy electron attachment leading to vibrational excitation or chemical bond cleavage of molecules has been extensively used to investigate the structure of molecules or molecular clusters as well as the states of the added electron [52], no dissociated products were observed in our AIMD simulations on bulk  $\text{scCO}_2$  with a zero-energy EE. This indicates that

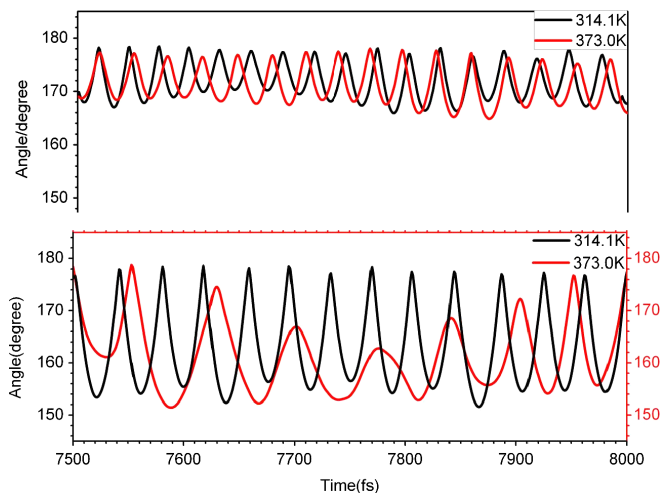


FIG. 6 (color online). Oscillations of the bending angle of two  $\text{CO}_2$  that do not participate in (upper panel) and participate in (lower panel) binding the EE, extracted from the AIMD simulations on  $\text{EE@scCO}_2$  at 314.1 (heavy black curve) and 373.0 K (light black curve), respectively. The average oscillation periods for the former are about 30 fs ( $\sim 28$  fs/373.0 K versus  $\sim 31$  fs/314.1 K), shorter than those of the latter ( $\sim 60$  fs/373.0 K versus  $\sim 40$  fs/314.1 K).

the stretching vibration is not a main contributor to the stabilization of the absorbed EE, and steady absorption of a zero-energy electron in  $\text{scCO}_2$  does not lead to vibrational excitation or to C–O bond cleavage, in agreement with the experimental observation of large dissociation energy ( $>4.0$  eV) of  $\text{CO}_2^-$  [26].

In summary, we have shown that after an EE is absorbed in  $\text{scCO}_2$ , various diffuse states and families of localized states are repeatedly observed. All these states convert from one to another through continuous breathing oscillations and core-switching pathways, with occasional dual-core intermediate states. All of the observed oscillations are attributed to the electron-impacted bending vibration of the core  $\text{CO}_2$ , and the core-switching is controlled by thermal fluctuations of the solvent.

In contrast with cluster-based results, where various  $(\text{CO}_2)_n$ -cored localized state structures were found, our AIMD simulations reveal not only localized states corresponding to the clustering structures, but also diffuse states corresponding to a conduction band structure, which occurs for about half the trajectory time. Frequent and fast conversions among the diffuse and localized states suggest that an EE has high mobility in  $\text{scCO}_2$ , in agreement with previous experimental conclusions, and is distinctly different from EE diffusion in polar liquids, such as water, which occurs on a much slower time scale [53]. Finally, we note that there has been great activity in the area of ultrafast 2D IR vibrational echo spectroscopy [54] that could be an appropriate probe of EE effects on  $\text{scCO}_2$  vibrational modes.

Acknowledgments for support of this work are made to NSFC (20633060, 20973101), NCET, and the Independent

Innovation Foundation of SDU (2009JC020), and also to the Shanghai Supercomputer Center, HPCC of SDU, and MCBILIN at MSU.

\*To whom correspondence should be addressed.

byx@sdu.edu.cn

- [1] E. J. Hart and J. W. Boag, *J. Am. Chem. Soc.* **84**, 4090 (1962).
- [2] J. P. Keene, *Nature (London)* **197**, 47 (1963).
- [3] D. H. Paik, I. R. Lee, D. S. Yang, J. S. Baskin, and A. H. Zewail, *Science* **306**, 672 (2004).
- [4] J. M. Herbert and M. Head-Gordon, *Proc. Natl. Acad. Sci. U.S.A.* **103**, 14282 (2006).
- [5] S. H. Simon, *Science* **324**, 1022 (2009).
- [6] R. E. Larsen, W. J. Glover, and B. J. Schwartz, *Science* **329**, 65 (2010).
- [7] K. D. Jordan and M. A. Johnson, *Science* **329**, 42 (2010).
- [8] M. Boero, M. Parrinello, K. Terakura, T. Ikeshoji, and C. C. Liew, *Phys. Rev. Lett.* **90**, 226403 (2003).
- [9] J. Stähler, M. Mehlhorn, U. Bovensiepen, M. Meyer, D. O. Kusmierik, K. Morgenstern, and M. Wolf, *Phys. Rev. Lett.* **98**, 206105 (2007).
- [10] D. Nordlund, H. Ogasawara, H. Bluhm, O. Takahashi, M. Odellius, M. Nagasono, L. G. M. Pettersson, and A. Nilsson, *Phys. Rev. Lett.* **99**, 217406 (2007).
- [11] F. Baletto, C. Cavazzoni, and S. Scandolo, *Phys. Rev. Lett.* **95**, 176801 (2005).
- [12] C. Desfrancois, Y. Bouteiller, J. P. Schermann, D. Radisic, S. T. Stokes, K. H. Bowen, N. I. Hammer, and R. N. Compton, *Phys. Rev. Lett.* **92**, 083003 (2004).
- [13] M. Mitsui, N. Ando, S. Kokubo, A. Nakajima, and K. Kaya, *Phys. Rev. Lett.* **91**, 153002 (2003).
- [14] M. Smyth and J. Kohanoff, *Phys. Rev. Lett.* **106**, 238108 (2011).
- [15] O. Marsalek, F. Uhlig, T. Frigato, B. Schmidt, and P. Jungwirth, *Phys. Rev. Lett.* **105**, 043002 (2010).
- [16] Z. P. Wang, L. Zhang, X. H. Chen, R. I. Cukier, and Y. X. Bu, *J. Phys. Chem. B* **113**, 8222 (2009).
- [17] Z. P. Wang, L. Zhang, R. I. Cukier, and Y. X. Bu, *Phys. Chem. Chem. Phys.* **12**, 1854 (2010).
- [18] V. Stastny and D. M. Rudkevich, *J. Am. Chem. Soc.* **129**, 1018 (2007).
- [19] D. Lee, J. C. Hutchison, J. M. DeSimone, and R. W. Murray, *J. Am. Chem. Soc.* **123**, 8406 (2001).
- [20] M. Motiei, Y. R. Hacoheh, J. Calderon-Moreno, and A. Gedanken, *J. Am. Chem. Soc.* **123**, 8624 (2001).
- [21] C. N. Field, P. A. Hamley, J. M. Webster, D. H. Gregory, J. J. Titman, and M. Poliakoff, *J. Am. Chem. Soc.* **122**, 2480 (2000).
- [22] S. Cummings, K. Trickett, R. Enick, and J. Eastoe, *Phys. Chem. Chem. Phys.* **13**, 1276 (2011).
- [23] J. Leclaire, G. Husson, N. Devaux, V. Delorme, L. Charles, F. Ziarelli, P. Desbois, A. Chaumonnot, M. Jacquin, F. Fotiadu, and G. Buono, *J. Am. Chem. Soc.* **132**, 3582 (2010).
- [24] O. Kajimoto, *Chem. Rev.* **99**, 355 (1999).
- [25] J. G. Stevens, R. A. Bourne, M. V. Twigg, and M. Poliakoff, *Angew. Chem., Int. Ed.* **49**, 8856 (2010).
- [26] K. Takahashi, S. Sawamura, N. M. Dimitrijevic, D. M. Bartels, and C. D. Jonah, *J. Phys. Chem. A* **106**, 108 (2002).
- [27] K. Itoh, A. Muraoka, K. Watanabe, T. Nagata, M. Nishikawa, and R. A. Holroyd, *J. Phys. Chem. B* **108**, 10177 (2004).
- [28] I. A. Shkrob and M. C., Jr. Sauer, *J. Phys. Chem. B* **105**, 4520 (2001).
- [29] N. M. Dimitrijevic, K. Takahashi, D. M. Bartels, C. D. Jonah, and A. D. Trifunac, *J. Phys. Chem. A* **104**, 568 (2000).
- [30] I. A. Shkrob, M. C. Sauer, C. D. Jonah, and K. Takahashi, *J. Phys. Chem. A* **106**, 11855 (2002).
- [31] I. A. Shkrob, *J. Phys. Chem. A* **106**, 11871 (2002).
- [32] R. Angamuthu, P. Byers, M. Lutz, A. L. Spek, and E. Bouwman, *Science* **327**, 313 (2010).
- [33] R. Banerjee, A. Phan, B. Wang, C. Knobler, H. Furukawa, M. O’Keeffe, and O. M. Yaghi, *et al.*, *Science* **319**, 939 (2008).
- [34] L. G. Wang, S. J. Pennycook, and S. T. Pantelides, *Phys. Rev. Lett.* **89**, 075506 (2002).
- [35] I. I. Fabrikant and H. Hotop, *Phys. Rev. Lett.* **94**, 063201 (2005).
- [36] W. Vanroose, Z. Zhang, C. W. McCurdy, and T. N. Rescigno, *Phys. Rev. Lett.* **92**, 053201 (2004).
- [37] T. Sommerfeld and T. Posset, *J. Chem. Phys.* **119**, 7714 (2003).
- [38] S. Denifl, V. Vizcaino, T. D. Märk, E. Illenberger, and P. Scheier, *Phys. Chem. Chem. Phys.* **12**, 5219 (2010).
- [39] T. Sommerfeld, H. D. Meyer, and L. S. Cederbaum, *Phys. Chem. Chem. Phys.* **6**, 42 (2004).
- [40] J. W. Shin, N. I. Hammer, and M. A. Johnson, *J. Phys. Chem. A* **109**, 3146 (2005).
- [41] R. Mabbs, E. Surber, L. Velarde, and A. Sanov, *J. Chem. Phys.* **120**, 5148 (2004).
- [42] K. E. Anderson, S. L. Mielke, J. I. Siepmann, and D. G. Truhlar, *J. Phys. Chem. A* **113**, 2053 (2009).
- [43] S. Balasubramanian, A. Kohlmeyer, and M. L. Klein, *J. Chem. Phys.* **131**, 144506 (2009).
- [44] M. Saharay and S. Balasubramanian, *J. Chem. Phys.* **120**, 9694 (2004).
- [45] M. Saharay and S. Balasubramanian, *J. Phys. Chem. B* **111**, 387 (2007).
- [46] R. Ishii, S. Okazaki, O. Odawara, I. Okada, M. Misawa, and T. Fukunaga, *Fluid Phase Equilib.* **104**, 291 (1995).
- [47] R. Ishii, S. Okazaki, I. Okada, M. Furusaka, N. Watanabe, M. Misawa, and T. Fukunaga, *J. Chem. Phys.* **105**, 7011 (1996).
- [48] All simulations were done with the DMOL3 package, as implemented in CERIUS2 version 4.6 Accelrys Inc., San Diego, CA.
- [49] B. Delley, *J. Chem. Phys.* **113**, 7756 (2000).
- [50] B. Delley, *J. Phys. Chem.* **100**, 6107 (1996).
- [51] See Supplemental Material at <http://link.aps.org/supplemental/10.1103/PhysRevLett.108.207601> for all AIMD simulation results, calculated UV absorption, IR vibrational spectra, orbital characters, and clustering effect, etc.
- [52] H. Hotop, M.-W. Ruf, M. Allan, and I. I. Fabrikant, *Adv. At. Mol. Opt. Phys.* **49**, 85 (2003).
- [53] K. H. Schmidt, P. Han, and D. M. Bartels, *J. Phys. Chem.* **96**, 199 (1992).
- [54] J. Zheng, K. Kwak, and M. D. Fayer, *Acc. Chem. Res.* **40**, 75 (2007).